ISSN 2070-0482, Mathematical Models and Computer Simulations, 2012, Vol. 4, No. 6, pp. 552–559. © Pleiades Publishing, Ltd., 2012.
Original Russian Text © T.G. Elizarova, M.A. Istomina, N.K. Shelkovnikov, 2012, published in Matematicheskoe Modelirovanie, 2012, Vol. 24, No. 4, pp. 107–116.

Numerical Simulation of Solitary Wave Generation in a Wind–Water Annular Tunnel

T. G. Elizarova, M. A. Istomina, and N. K. Shelkovnikov

Keldysh Institute of Applied Mathematics, Russian Academy of Sciences, Miusskaya pl. 4, Moscow, 125047 Russia
e-mail: telizar@mail.ru
Faculty of Physics, Moscow State University, Moscow, 119991 Russia

Received August 11, 2011

Abstract—We briefly describe laboratory experiments demonstrating wind–water solitary wave generation in a wind–water annular tunnel. A mathematical model of this phenomenon is constructed in the context of a shallow-water approximation. The finite-difference algorithm for solving the system is based on regularized shallow-water equations. For the first time, we obtain a numerical solution of the wind–water solitary wave that is qualitatively consistent with the experimental data.

Keywords: wind–water solitary wave, shallow-water equations, quasi-gas dynamic equations, regularized shallow-water equations

DOI: 10.1134/S2070048212060051

INTRODUCTION

Among wave motions in seas and oceans, the emergence and behavior of large-amplitude solitary waves (called in the literature extreme, or giant, waves) are of great interest. A number of publications call them killer waves. There has been much evidence that ships and drilling platforms encounter unusual waves with a height greater than the surrounding waves and an unexpected time of their emergence and disappearance [1–4]. Similar to tsunami waves of seismic origin, the height of these waves when approaching the coast sharply increases and can cause significant damage to the coast.

According to modern concepts and observational experience, in some cases, these waves can be generated by wind and act as a solitary wave or a group of solitons. In this case, a soliton is meant to be a stable solitary wave that has some properties of particles when these waves interact with one another or are reflected from obstacles [5, 6].

The mechanism of the generation of wave–wind solitons has not been fully understood because studying solitons in the real world is very difficult. This phenomenon was investigated experimentally [2, 3]; its theoretical analysis was based on the Korteweg–de Vries equations and nonlinear Schrödinger-type equations [4]. Both theoretical models presuppose the existence of soliton-type solutions.

In this study, we show for the first time that it is possible to conduct a direct numerical simulation of the emergence of an isolated wind–wave soliton on the basis of shallow-water equations. The numerical algorithm is based on the use of regularized equations [7–9]. The main parameters of the mathematical model yielding the results described below are consistent with the laboratory experimental data [2, 3].

1. DESCRIPTION OF THE EXPERIMENT

According to [2, 3], the experimental setup is an annular hydrochannel with external and internal diameters $R_1 = 2.02$ m and $R_2 = 1.65$ m, respectively. The height of the channel is 0.4 m. Hereinafter, all quantities will be in SI units. The side walls of the channel are made of organic glass, which makes it possible to observe and take video/photo shootings through these glasses.

The airflow from the fan is blown into the space between the water surface and channel cover. The fan is located at the center of the channel, and the airflow, controlled by a special device, enters into the mouths through hermetic flexible hoses. The lower part of the mouth has a bottom allowing the airflow to be aligned and enter the channel almost horizontally. The wind speed can be varied from 3 to 15 m/s. A photo of the experimental setup is shown in Fig. 1.

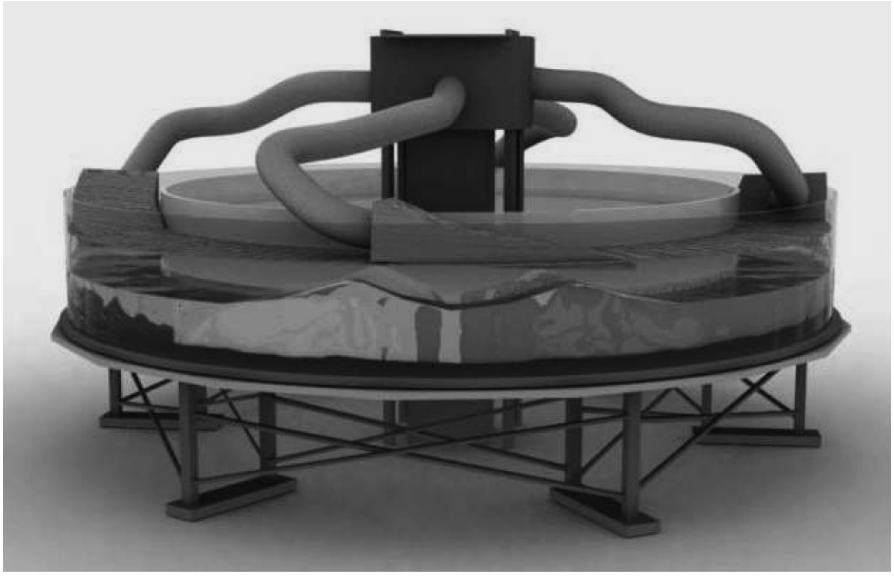

Fig. 1. Photo of the experimental setup. The annular channel.

Fig. 2. Photo of the experimental setup. A fragment showing the presence of two solitons.

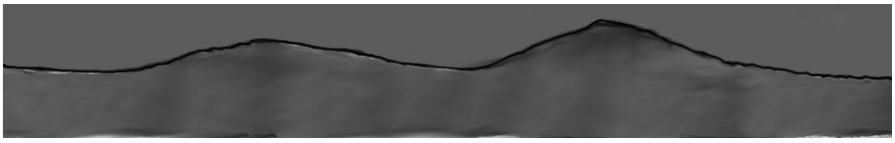

Fig. 3. Photo showing two solitons in the annular channel.

The waves were recorded using four string wave recorders; the signal from these recorders goes to the input of the ADC-board of a computer. In addition, five video cameras located along the whole length of the channel were used.

Solitons emerged when the depth was changed from 0.05 to 0.14 m and the wind speed was changed from 12 to 15 m/s.

Under these conditions, the generation of solitary waves involves the following main stages. When the fan is turned on and after some time of settling, the fluid surface involves a sequence of several emerging waves of different sizes. The characteristic features of this first stage may differ somewhat from one experiment to another and depend on wind speed, water depth, and its surface properties, as well as the presence of impurities in it.

As a result of the nonlinear interaction of these structures, the large waves overtake and absorb the small waves, and this absorption is accompanied by a complex process of their interaction. One of the stages of this process is the formation of two solitons in the channel (see Figs. 2 and 3). This leads to the formation of a single pulse, the leeward slope of which is steeper and the windward slope is stretched (see Fig. 4). With a further steepening of the leading front, the soliton partially collapses but keeps its general shape. This resulting pulse is stable and moves with a constant velocity and amplitude until the wind effect changes. When the fan is turned off, the motion of the soliton slows and is completely attenuated.

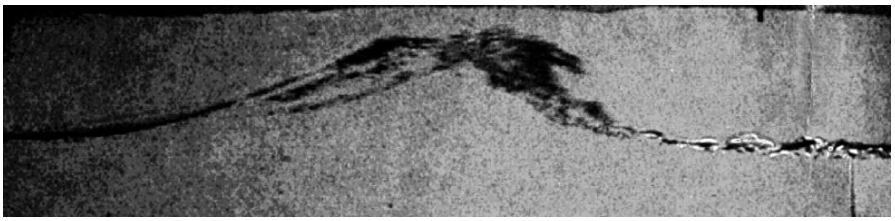

Fig. 4. Wind soliton in the annular channel. One can see that the leading front is partially collapsed. The actual size of the flow field is approximately 1 : 0.2 m.

2. MATHEMATICAL MODEL AND FINITE-DIFFERENCE ALGORITHM

The aerohydrochannel width is around 0.4 m and its length is 5.76 m for an average radius of $R = (R_1 + R_2)/2$, which is substantially greater than the channel width. Neglecting transverse disturbances in the liquid, we describe the wave phenomena in terms of one-dimensional planar equations of hydrodynamics. The liquid height in the channel is around 0.1 m, and the soliton height is also not more than 0.15 m. The latter makes it possible to use shallow-water equations for a planar one-dimensional flow as a mathematical model of the process. Taking into consideration the wind strength and the fluid friction at the channel wall, the system of shallow-water equations has the form

$$\frac{\partial h}{\partial t} + \frac{\partial}{\partial x} hu = 0, \quad \frac{\partial}{\partial t} hu + \frac{\partial}{\partial x} hu^2 + \frac{\partial}{\partial x}\left(\frac{gh^2}{2}\right) = h\left(f - g\frac{\partial b}{\partial x}\right) - \mu u|u|. \tag{1}$$

Here, h and u are the fluid height and velocity, respectively; b is the bottom topography; and g is the gravitational acceleration. In this case, the channel bottom topography is flat; therefore, we take $b = 0$ in the calculations. The force f acting on the fluid surface is proportional to wind speed U, $f = \gamma U^2$, where $U =$ 3–15 m/s. The wind friction coefficient γ is measured experimentally. Its value depends on many parameters, including the state of the fluid surface and the wind speed. For example, the experiments performed for the Black Sea and Sea of Azov yield $\gamma \sim 10^{-2}$ ([12], p. 302) and $\gamma \sim 10^{-5}$, respectively. Since the wind friction coefficient for the given experiment was estimated to be in the range between 0.01 and 0.2, we consider the value of f as a parameter of the problem. Another parameter is the coefficient of friction μ at the wall and bottom of the channel (the value of this coefficient for these experiments is unknown).

In line with the experimental conditions, as the initial conditions, we take the disturbance of the fluid surface profile in the form of a level elevation in some small area. The boundary conditions are taken to be the periodicity conditions for the fluid velocity and height, which reflects the fluid flow in the annular channel.

To solve problem (1) numerically, we use a regularized system of shallow-water equations [7–9]. This system was derived from averaging the shallow-water equations over a small interval of time and as a barotropic approximation of quasi-gas dynamic equations [10, 11]. These equations contain regularizing (or smoothing) terms allowing one to use simple and efficient numerical algorithms for their implementation. These algorithms are efficient in the calculation of nonstationary or oscillatory motions of a gas and liquid. Detailed testing of the numerical algorithm for one-dimensional flows in a shallow-water approximation can be found in [9].

The regularized system of shallow-water equations for one-dimensional flows taking into account the external forces and bottom irregularities has the form [8]

$$\frac{\partial h}{\partial t} + \frac{\partial}{\partial x} j_m = 0, \quad \frac{\partial}{\partial t} hu + \frac{\partial}{\partial x} j_m u + \frac{\partial}{\partial x}\left(\frac{gh^2}{2}\right) = \left(h - \tau\frac{\partial hu}{\partial x}\right)\left(f - g\frac{\partial b}{\partial x}\right) - \mu u|u| + \frac{\partial}{\partial x}\Pi,$$

$$j_m = h(u - w), \quad w = \frac{\tau}{h}\left(\frac{\partial hu^2}{\partial x} + gh\frac{\partial h}{\partial x} + gh\frac{\partial b}{\partial x} - hf\right), \tag{2}$$

$$\Pi = \tau uh\left(u\frac{\partial u}{\partial x} + g\frac{\partial h}{\partial x} + g\frac{\partial b}{\partial x} - f\right) + \tau gh\left(u\frac{\partial h}{\partial x} + h\frac{\partial u}{\partial x}\right),$$

where τ is the parameter of regularization (or smoothing).

We introduce a uniform grid with respect to the x coordinate with step h_x and node coordinates x_i, as well as a grid with respect to time with step Δt. The system of equations (2) is solved on the basis of a central difference scheme that is explicit in time. The values of gas dynamic variables are determined in grid cells. The values of fluxes are determined in half-integer cells. The difference approximation of Eqs. (2) has the form

$$\hat{h}_i = h_i - \Delta t \frac{j_{m,i+1/2} - j_{m,i-1/2}}{h_x}, \tag{3}$$

$$\begin{aligned}\hat{u}_i = \frac{1}{\hat{h}_i}\Bigg(h_i u_i - \Delta t \frac{j_{m,i+1/2}u_{i+1/2} - j_{m,i-1/2}u_{i-1/2}}{h_x} - \Delta t \frac{g}{2}\frac{h_{i+1/2}^2 - h_{i-1/2}^2}{h_x} \\ - \Delta t \mu u_i |u_i| + \Delta t f_i \Bigg(\frac{h_{i+1/2} - h_{i-1/2}}{2} - \tau_i \frac{h_{i+1/2}u_{i+1/2} - h_{i-1/2}u_{i-1/2}}{h_x}\Bigg) + \Delta t \frac{\Pi_{i+1/2} + \Pi_{i-1/2}}{h_x}\Bigg),\end{aligned} \tag{4}$$

where the flux values in half-integer points are computed as

$$j_{m,i+1/2} = h_{i+1/2}(u_{i+1/2} - w_{i+1/2}), \tag{5}$$

$$w_{i+1/2} = \frac{\tau_{i+1/2}}{h_{i+1/2}}\Bigg(\frac{h_{i+1}u_{i+1}^2 - h_i u_i^2}{h_x} + g h_{i+1/2}\frac{h_{i+1} - h_i}{h_x} - h_{i+1/2} f_{i+1/2}\Bigg). \tag{6}$$

The finite-difference approximation of $\Pi_{i+1/2}$ is constructed similar to the formulas for the flux $w_{i+1/2}$. The symbol (^) indicates the value of the function at the upper time layer. The smoothing parameter is calculated as

$$\tau_{i+1/2} = \alpha \frac{h_x}{\sqrt{g h_{i+1/2}}}. \tag{7}$$

The stability and accuracy of the numerical algorithm depend on the smoothing parameter τ, where the numerical coefficient $0 < \alpha < 1$ is chosen from the conditions of accuracy and stability of the solution. The stability condition is given by the Courant condition

$$\Delta t = \beta \frac{h_x}{\sqrt{gh}}, \tag{8}$$

where the Courant number $0 < \beta < 1$ is chosen during the computation to ensure the stability of the scheme. The values of μ and f are considered as parameters of the problem.

3. NUMERICAL SIMULATION OF THE SOLITON FORMATION

The problem is considered in the domain $0 \le x \le L$, where $L = 6$ m. The initial conditions are chosen as the pulse of a width fitting the grid step h_x, $h(x, 0) = 0.2$. At the initial time, the fluid is fixed: $u(x, 0) = 0$.

The periodic boundary conditions $u(x) = u(x + L)$ and $h(x) = h(x + L)$ are given in a difference form as

$$h(1) = h(N-1), \quad h(N) = h(2), \quad u(1) = u(N-1), \quad u(N) = u(2). \tag{9}$$

Here, N is the number of points of the difference grid in space, $i = 1, \ldots N$. The time step is calculated as

$$\Delta t = \beta \frac{h_x}{\sqrt{g h_{\max}(x, 0)}}.$$

This problem was numerically investigated through a series of calculations where the magnitude of the external force f and the coefficient of friction at the wall were varied in the ranges 0–100 and 0.01–100, respectively. The grid parameters α and β varied in the range 0.01–1. Most calculations were performed on the grid with step $h_x = 0.01$. The numerical experiments indicated that the numerical algorithm for the given problem is stable when the regularizer is chosen with a coefficient of $\alpha \sim 0.1$–0.3 and a Courant number $\beta \sim 0.05$–0.1. With increasing α, the solution becomes highly smoothed; with its reduction, the solution becomes unstable. In this case, in order to retain computational stability, the time step needs to

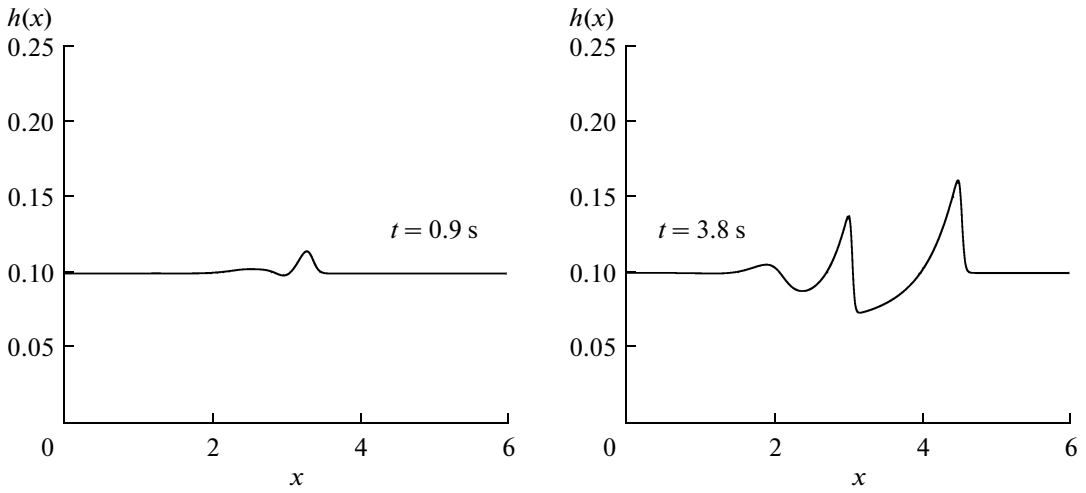

Fig. 5. Height $h(x)$ at $t = 0.9$ and 3.8 s.

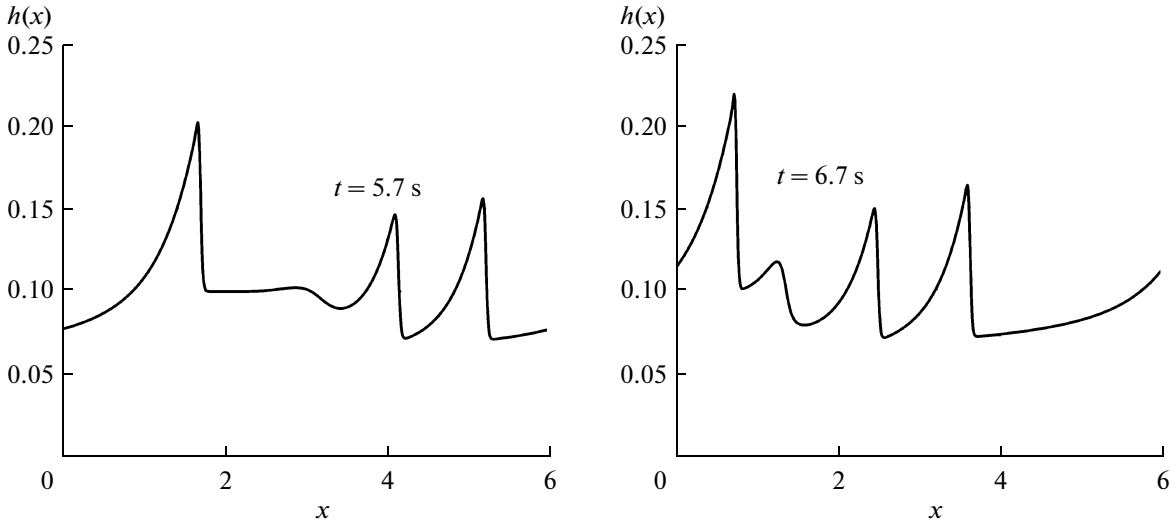

Fig. 6. Height $h(x)$ at $t = 5.7$ and 6.7 s.

be reduced. The numerical scheme is conditionally stable; therefore, when the Courant number goes below the above-mentioned values, the numerical solution is independent of the time step.

Out of a total number of 70 model runs, 11 revealed soliton solutions. In the remaining cases, the initial disturbance in the fluid level faded or a nonstationary flow was generated without solitons. The calculations indicated that a single soliton was generated when the ratio of wind strength to the friction coefficient was of the form $f/\mu \sim 50$–100 m/s^2. The soliton formation time is 10 to 60 s; the total time of calculations was $t = 600$ s. The solitons obtained in different calculations differed somewhat in their shape, speed, and the way in which they settled.

A typical example with a soliton solution is shown in Figs. 5–9. Here, one can see the development of a single soliton obtained for $\mu = 0.1, f = 0.1$, and the parameters of the numerical algorithm $h_x = 0.01$, $\alpha = 0.1$, and $\beta = 0.05$. One can see the development of a disturbance of the fluid surface (Figs. 5 and 6), its further evolution with the formation of two solitons of different sizes, and the subsequent interaction between these solitons, during which the soliton with a higher amplitude overtakes and absorbs the smaller size soliton (Figs. 7 and 8). As a result, a single undamped wave is generated. This process of soliton formation is fully consistent with the experimental observations described in detail in [1–3] and illustrated

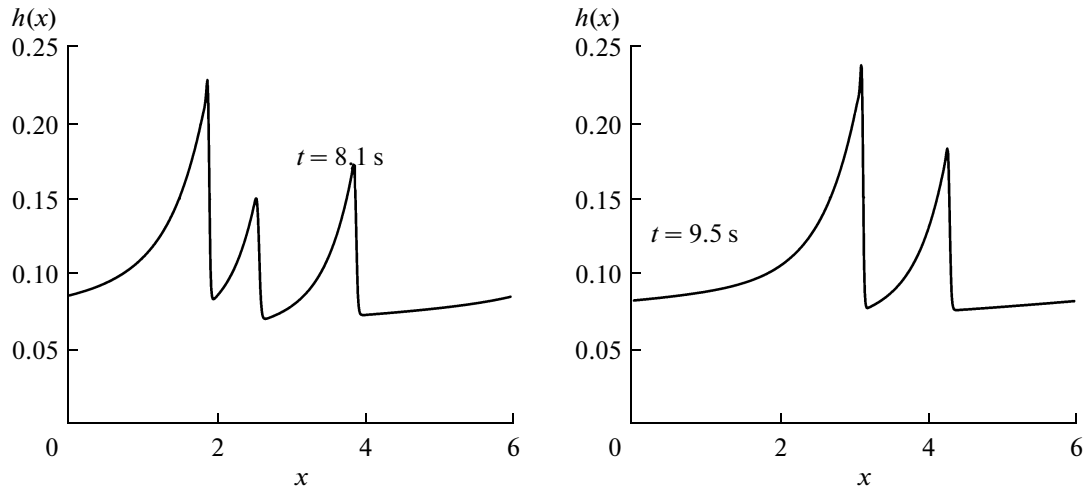

Fig. 7. Height $h(x)$ at $t = 8.1$ and 9.5 s.

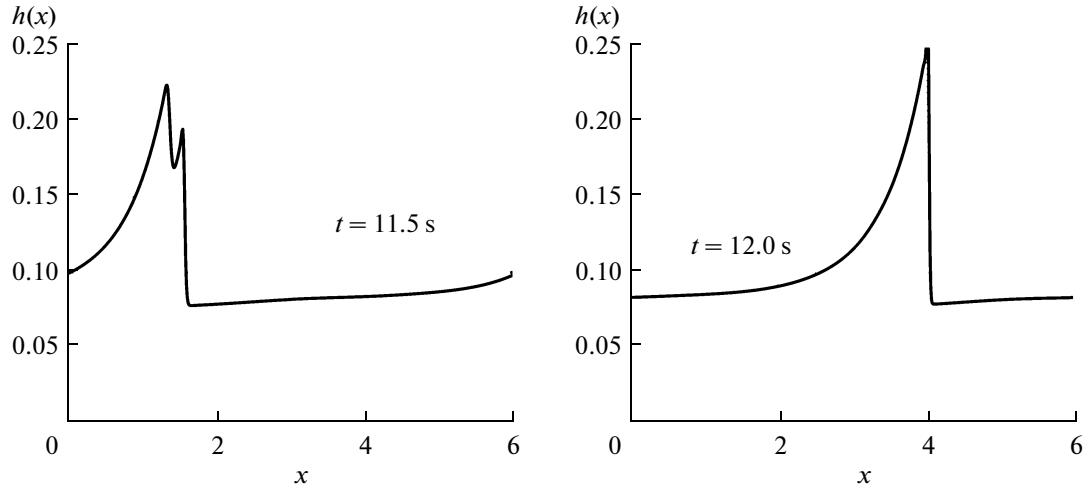

Fig. 8. Height $h(x)$ at $t = 11.5$ and 12.0 s.

in Figs. 2–4. The windward front of the resulting soliton is flatter and the leeward front is steeper (Fig. 8); the soliton height is around 0.15 m, which is also consistent with the experimentally observed pattern (Fig. 4).

The fluid velocity at time $t = 12$ s is shown in Fig. 9. It can be seen that the soliton moves faster than the liquid on the surface of which it has been formed. According to theoretical estimates made in the Korteweg–de Vries equation model, the soliton velocity C_s for the case of a fixed fluid is approximately expressed by the ratio [1–3]

$$C_s = c\left(1 + \frac{h_c}{2H}\right), \tag{10}$$

where $c = \sqrt{gH}$ is the Lagrangian velocity of waves, h_c is the soliton height, and H is the fluid depth.

Figure 9 shows that the soliton velocity with respect to the moving fluid is $C_s \approx 1.6$. According to Fig. 8, $h_c \sim 0.15$, $H \sim 0.1$; i.e., $1 + h_c/2H = 1.75$, $c \approx 1$ and, thus, estimate (10) yields $C_s \sim 1.75$, which is qualitatively consistent with the calculation data.

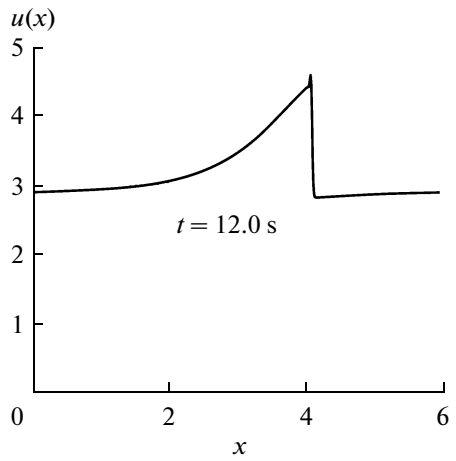

Fig. 9. Soliton velocity $u(x)$ at $t = 12.0$ s.

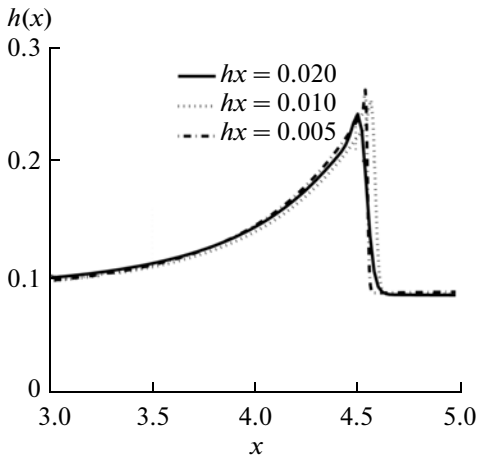

Fig. 10. The grid effect. The shape of the soliton in the steady state $h(x)$ for $f = 10.0$, $\mu = 0.1$, $\alpha = 0.1$, and $\beta = 0.1$ for $h_x = 0.025$, 0.010 and 0.005.

As in the experiment, the pulse rapidly decays without an external force. If a depression rather than elevation of the fluid level is used as the initial condition, no soliton is generated in both the laboratory and numerical experiments.

The existence of a soliton is conditioned by a careful balance of the hydrodynamic nonlinear processes that lead to an increase in the steepness of the leading front of the wave and the dispersion and viscous processes that diffuse a solitary wave (see, for example, [5, 6]). It is evident that the viscous effects play an important role in the formation of a soliton solution.

The difference scheme used by the authors has artificial dissipation proportional to the step of the spatial grid. Figure 10 shows steady-state soliton profiles obtained from calculations on grids with steps $h_x = 0.005$, 0.01, and 0.025. For all the three grids, there exist a soliton solution; in this case, the leading front of the soliton on the finest grid with $h_x = 0.005$ turns out to be slightly steeper and its maximum slightly higher than in the calculations on the coarser grids. In general, the shape of the soliton depends weakly on the grid step, which testifies to the fact that the numerical dissipation of the difference scheme is small.

Thus, it has been shown for the first time that the model based on shallow-water equations with wind strength and friction force makes it possible to obtain a numerical solution of the form of a wind soliton. The process of soliton formation, as well as the form and nature of its formation and motion, is consistent with the experimental data for the wind–wave channel. This finding makes a significant contribution to the understanding of the mechanism of the formation of wave–wind solitary waves.

CONCLUSIONS

This paper provides a brief description of experiments in an aerohydrochannel. Mathematical model of wind–wave solitons is constructed for the first time within a shallow-water approximation.

The model is based on shallow-water equations for a one-dimensional planar flow, taking into consideration the friction force at the wall and the wind effect. The numerical simulation is based on regularized equations. The resulting solutions correctly reflect the characteristics of the generation and behavior of solitary waves observed in the experiment.

The investigation of the generation mechanism of wind–wave solitons in a laboratory experiment is a rather difficult task; in natural conditions, it is almost impossible. Therefore, the description of the given phenomenon in the approximation of shallow-water equations and its investigation with the help of numerical experiments is of great interest.

ACKNOWLEDGMENTS

This study was supported by the Russian Foundation for Basic Research, project no. 10-01-00136.

REFERENCES

1. B. V. Levin and M. A. Nosov, *Physics of Tsunamis* (Yanus-K, Moscow, 2005) [in Russian].
2. O. A. Glebova, Al. V. Kravtsov, and N. K. Shelkovnikov, "Experimental and Numerical Study of Wind Solitary Waves on Water," Izv. Akad. Nauk, Ser. Fiz. **66** (12), 1727–1729 (2002).
3. N. K. Shelkovnikov, "Induced Soliton in a Fluid," JETP Lett. **82** (10), 638–641 (2005).
4. Al. N. Kravtsov, V. V. Kravtsov, and N. K. Shelkovnikov, "A Numerical Experiment on the Modeling of Solitary Waves on the Surface of a Fluid in an Annular Channel," Comput. Math. Math. Phys. **44** (3), 529–531 (2004).
5. R. K. Dodd, J. C. Eilbeck, J. D. Gibbon, et al., *Solitons and Nonlinear Wave Equations* (Academic Press, London, 1982; Mir, Moscow, 1988).
6. A. N. Volobuev, V. I. Koshev, and E. S. Petrov, *Biophysical Principles of Geodynamics* (Moscow, 2009) [in Russian].
7. T. G. Elizarova and O. V. Bulatov, "Regularized Shallow Water Equations and a New Method of Simulation of the Open Channel Flows," Comput. Fluids **46** (1), 206–211 (2011).
8. O. V. Bulatov and T. G. Elizarova, "Regularized Shallow Water Equations and an Efficient Method for Numerical Simulation of Shallow Water Flows," Comput. Math. Math. Phys. **51** (1), 160–173 (2011).
9. T. G. Elizarova, A. A. Zlotnik, and O. V. Nikitina, "Simulation of One-Dimensional Shallow-Water Flows using Regularized Equations," Preprint No. 33 (Keldysh Inst. Appl. Math., Moscow, 2011).
10. T. G. Elizarova, *Quasi-Gas Dynamic Equations and Methods for the Computation of Viscous Flow* (Nauchnyi mir, Moscow, 2007) [in Russian]. English Translation: Springer 2009.
11. Yu. V. Sheretov, *Dynamics of Continuous Media in Spatial and Temporal Averaging* (RC Dynamics, Moscow–Izhevsk, 2009) [in Russian].
12. G. I. Marchuk, *Mathematical Modeling in the Problem of Environment* (Nauka, Moscow, 1982) [In Russian].